Introduction to UCLA-LES

Version 3.2.1

Bjorn Stevens

August 12, 2013

Contents

1. Introduction

b. *History and Contributions*

This code grew out of the cloud and meso-scale modeling projects directed by Professors William R. Cotton and Roger Pielke in the Department of Atmospheric Science at Colorado State University. Most of the actual development in these projects was performed by Craig Tremback, now of Mission Research Inc., Robert L. Walko, now at Rutgers, Greg Tripoli, now at the University of Wisconsin, and Jim Edwards, now at NCAR with IBM, their collective efforts are reflected in many respects in this particular code — a descendant of the code they developed. The actual development of this code was mostly done by myself with important contributions by Jim Edwards (the initial parallelization); Graham Feingold, Verica Savic-Jovcic and Axel Seifert (microphysics); Hsin-Yuan Huang also has implemented and tested a variety of subgrid models, which are not incorporated in this distribution.

2. Physical Model

a. *Model Equations*

Prognostic variables include the three components of the wind ($u_i \equiv \{u, v, w\}$); the liquid-water potential temperature, θ_l; the total-water mixing ratio, q_t; and, as the case may be, an arbitrary number of scalars, ϕ_m, in support of microphysical processes, more sophisticated sub-grid models, or studies of tracer transport or chemical processes. Grid-scale quantities are denoted by an overbar. Roughly speaking they can be thought of as grid-scale avaraged quantities where the exact term of the averaging operator is implicitly defined by the numerics, and unknown.

The form of the equations solved by the model are (in tensor notation) as follows:

$$\frac{\partial \bar{u}_i}{\partial t} = -\bar{u}_j \frac{\partial \bar{u}_i}{\partial x_j} - c_p \Theta_0 \frac{\partial \bar{\pi}}{\partial x_i} + \frac{g \bar{\theta}_v''}{\Theta_0} \delta_{i3} + f_k(\bar{u}_j - V_{g,j})\epsilon_{ijk} + \frac{1}{\rho_0} \frac{\partial(\rho_0 \tau_{ij})}{\partial x_j}, \tag{1}$$

$$\frac{\partial \bar{\phi}}{\partial t} = -\bar{u}_j \frac{\partial \bar{\phi}}{\partial x_j} + \frac{1}{\rho_0} \frac{\partial(\rho_0 \gamma_{\phi j})}{\partial x_j} + \frac{\partial F_\phi}{\partial x_j} \delta_{j3}, \tag{2}$$

subject to the anelastic continuity equation

$$\frac{\partial(\rho_0 u_i)}{\partial x_i} = 0 \tag{3}$$

and an equation of state which we take to be the ideal gas law for a perfect mixture:

$$\theta_v = \theta \left(1 + (R_v/R_d - 1)q_t - (R_v/R_d)q_l\right). \tag{4}$$

In the above $\bar{\pi} = (\bar{p}/p_{00})^{R_d/c_p}$ is the exner function, it measures the dynamic pressure perturbation. F_ϕ denotes a flux whose divergence contributes to the evolution of ϕ (for instance radiation in the case $\phi = \theta_l$), $f_k = \{0, 0, f\}$ is the Coriolis parameter, $V_{g,j}$ is the geostrophic wind, and

$$\tau_{ij} \equiv \overline{u_i u_j} - \bar{u}_i \bar{u}_j \quad \text{and} \quad \gamma_{\phi j} \equiv \overline{\phi u_j} - \bar{\phi} \bar{u}_j \tag{5}$$

denote the sub-grid fluxes. In (2) ϕ denotes an arbitrary scalar. Depending on the level of microphysical complexity this can include θ_l and q_t or an arbitrary number of additional variables, for instance to represent microphysical habits or categories. The symbols δ_{jk} and ϵ_{ijk} denote the Kronecker-delta and Levi-Civita symbol respectively.

The anelastic approximation solves for perturbations about a hydrostatic basic state of constant potential temperature, i.e.,

$$\frac{d\pi_0}{dz} = -\frac{g}{c_p \Theta_0}, \tag{6}$$

where subscript 0 denotes a basic state value, which depend only on z (Θ_0 being constant). This follows the set of equation introduced by Ogura and Phillip (1962). Note that through the division by Θ_0 in the buoyancy term, model results can be sensitive to the value chosen for Θ_0.

In equation (1) $\bar{\theta}_v''$ denotes the deviation of $\bar{\theta}_v$ from the basic-state Θ_0. Thus, a mean vertical acceleration can arise. For consistency of the thermodynamic fields this requires the introduction of a second pressure, π_1 :

$$\frac{d}{dz}(\pi_0 + \pi_1) = -\frac{g}{c_p \bar{\theta}_v}, \tag{7}$$

that contains the contribution of deviations from the Θ_0 reference state to the pressure. This pressure depends on time, and is updated in the code by finding the pressure that balances the mean accelerations, such that

$$\frac{d\pi_1}{dz} = \frac{\dot{\bar{w}}}{c_p \Theta_0}, \tag{8}$$

with $\pi_1(z = 0)$ fixed at its initial value.

The model represents the First Law of thermodynamics by (2) with $\phi = \theta_l$. Where we define θ_l as:

$$\theta_l = T\pi \exp\left(-\frac{q_l L_v}{c_p T}\right) \tag{9}$$

Hence the model satisfies an approximate form of the First Law, but one generally consistent with the overall level of approximation. In the above L_v, R_d, R_v, c_p and p_{00} are thermodynamic parameters which adopt standard values (see Table 1) as is g the gravitational acceleration.

Table 1: Default values of model constants

Constant	Value
p_{00}	10^5 Pa
R_d	287.04 J kg^{-1} K^{-1}
R_v	461.5 J kg^{-1} K^{-1}
c_p	1004 J kg^{-1} K^{-1}
L_v	2.5 $\times 10^6$ J kg^{-1}
Ω	7.292 $\times 10^{-5}$ s^{-1}
g	9.80 m s^{-1}

The continuity equation (3), applied after taking the density weighted divergence of (1), yields $\tilde{\pi}$ through the inversion of the Poisson equation:

$$\frac{\partial}{\partial x_i}\left(\rho_0 \frac{\partial \tilde{\pi}}{\partial x_i}\right) = \frac{1}{c_p \Theta_0}\left[\frac{\partial}{\partial x_i}\left(-\rho_0 \bar{u}_j \frac{\partial \bar{u}_i}{\partial x_j} + \frac{\rho_0 g \bar{\theta}_v''}{\Theta_0}\delta_{i3} + \rho_0 f_k(\bar{u}_j - u_{jg})\epsilon_{ijk} + \frac{\partial(\rho_0 \tau_{ij})}{\partial x_j}\right)\right],$$

(10)

b. *Parameterizations and Models*

i. Turbulence The sub-grid fluxes τ_{ij} and $\gamma_{\phi j}$ are not known explicitly and thus must be modeled. This constitutes the model closure. The basic or default form of the closure makes use of the Smagorinsky model, wherein

$$\tau_{ij} = -\rho_0 K_m D_{ij} \quad \text{and} \quad \gamma_{\phi j} = -\frac{K_m}{Pr}\frac{\partial \bar{\phi}}{\partial x_j},$$

(11)

where

$$D_{ij} = \frac{\partial \bar{u}_i}{\partial x_j} + \frac{\partial \bar{u}_j}{\partial x_i}$$

is the resolved deformation, K_m is the eddy viscosity, and Pr is an eddy Prandtl number. The Smagorinsky model calculates the eddy viscosity as

$$K_m = (C_s \ell)^2 S \sqrt{1 - \frac{Ri}{Pr}} \quad \text{where} \quad Ri = \frac{S^2}{N^2}$$

(12)

and

$$S^2 \equiv \frac{\partial \bar{u}_i}{\partial x_j} D_{ij} \quad \text{and} \quad N^2 = \frac{g}{\Theta_0}\frac{\partial \bar{\theta}_v}{\partial z}.$$

(13)

In the above C_s is the Smagorinsky constant and takes on values near 0.2, and

$$\ell^{-2} = (\Delta x \Delta y \Delta z)^{-2/3} + (z\kappa/C_s)^{-2},$$

where $\kappa = 0.35$ is the von Kármán constant in the model. The geometric averaging between a grid scale and a length scale proportional to the height above the surface allows $K_m/(u_* z)$ to approach κ in the neutral surface layer (the log-law).

Other options include Lagrangian averaged scale-dependent and scale-independent models (implemented by Hsin-Yuan Huang) the Deardorff-Lilly sub-grid turbulence kinetic energy (TKE) model, and for scalars the option of having all the dissipation carried by the numerics.

ii. Microphysics The model allows for a range of microphysical complexity. In the standard distribution a warm-rain microphysical scheme is implemented following the work of Seifert and Beheng (2001) as implemented in Stevens and Seifert (2008). In this scheme cloud droplets are assumed to be in equilibrium with a fixed (specified) concentration. Cloud, or rain, drops defined as liquid condensate with appreciable fall velocities are allowed to evolve under the action of the ambient flow and microphysical processes (auto-conversion, accretion, self-collection, sedimentation). The representation of these processes leads to the inclusion of two additional prognostic equations, one for rain mass the other for rain concentration.

A saturation adjustment scheme is also implemented in the model. This scheme has no rain category and diagnoses cloud drop mass concentrations by assuming homogeneity on the grid-scale and equilibrium thermodynamics. Sedimentation of cloud droplets can be implemented as a source term in the model, but is not a default.

The prognostic equations for the microphysical quantities used by the bulk (level 3, imcrtyp 2) model, may be written as follows

$$\frac{\partial \psi}{\partial t} + \mathbf{u} \cdot \nabla \psi - \nabla \cdot (K_\psi \nabla \psi) = -w_\psi \frac{\partial \psi}{\partial z} + \mathcal{K}_\psi + \mathcal{T}_\psi \tag{14}$$

where here ψ stands for a microphysical variable, in our case $\psi \in \{n_r, r_r\}$. The terms on the lhs represent dynamic processes, and K_ψ is the eddy diffusivity of ψ which we set to K_h the eddy diffusivity of heat. The rhs terms represent different classes of microphysical processes. From left to right these are: (i) sedimentation, with terminal velocity w_ψ; (ii) $\mathcal{K}_\psi$, the transformation of ψ due to kinetic processes; and (iii) $\mathcal{T}_\psi$, the transformation associated with thermodynamic processes, which given our assumption that condensation is carried entirely by the cloud droplets, includes only evaporation. Note that the microphysical literature often speaks of kinetic effects in terms of molecular kinetics. At the risk of confusing matters, here we use *kinetic* to describe microphysical transformations arising from the interactions among drops, namely effects associated with droplet collisions, such as coalescence or breakup.

The Seifert and Beheng (SB) model is centered around the idea that the size distributions of cloud droplets and rain drops can be described by separated (truncated) gamma distributions with a separation diameter, D_* of 80 microns. The gamma distribution can be written as

$$f(D) = N_0 D^\mu \exp(-D/D_p), \tag{15}$$

where D_p, is the mean diameter, and μ is the shape parameter. In the original formulation of the scheme cloud droplets were allowed to have $\mu > 0$, while μ was fixed to zero for rain drops. Here, motivated by Seifert (2008), and the study of Milbrandt and Yau (2005), the formulation is generalized to allow $\mu > 0$ for the rain-drop mode as well. Formally

$$n_r = \int_{D_*}^\infty f(D) \, \mathrm{d}D \quad \text{and} \quad r_r = \frac{\rho_l \pi}{6} \int_{D_*}^\infty D^3 f(D) \, \mathrm{d}D \tag{16}$$

where D_* is the critical size separating drops from droplets, and ρ_l is the density of liquid water. Given f, then the mean volume (or mass) diameter follows as

$$D_m = \left[\frac{1}{n_r} \int_{D_*}^\infty D^3 f(D) \right]^{1/3}, \tag{17}$$

and the mean diameter is

$$D_p = \frac{1}{n_r} \int_{D_*}^\infty D f(D) \tag{18}$$

For a gamma distribution with $D_* = 0$ the relationships among the different microphysical moments, or parameters, depends only on μ, for instance

$$D_p = [\frac{6r_r}{\pi \rho_w n_r} \frac{1}{(\mu+3)(\mu+2)(\mu+1)}]^{1/3} \quad \text{and} \quad N_0 = \frac{n_r}{\Gamma(\mu+1)} D_p^{-(\mu+1)}. \tag{19}$$

Because evaluating the integrals over $f(D)$ for $D_* \neq 0$ yields incomplete Gamma functions, which are computationally delicate to represent, D_* is often taken to zero when evaluating moments or parameters of the droplet distribution. In two-moment schemes μ usually enters as a parameter, although it can be allowed to vary as a function of the other moments. For instance, for many of our simulations we diagnose

$$\mu = 10(1 + \tanh(1200(D_m - 0.0014))) \tag{20}$$

so that for small D_m the drop size distribution becomes exponential.

Neglecting the effects of variable density (which can be justified for shallow clouds, and is here done solely for to streamline the discussion) the SB Model is as follows

$$\mathcal{K}_{r_r}^{(sb)} = a_{sb}\frac{r_c^4}{N_c^2}\phi_{cc}(\varepsilon) + b_{sb}r_c r_r \phi_{cr}(\varepsilon) \tag{21}$$

$$\mathcal{K}_{n_r}^{(sb)} = \frac{\rho_l \pi}{6}D_*^3\left(a_{sb}\frac{r_c^4}{N_c^2}\phi_{cc}(\varepsilon)\right) - b_{sb}n_r r_r \beta(D_m). \tag{22}$$

Here a_{sb} is a constant (Table 2) which is derived using the Long (1974) Kernel for collection and incorporates the assumed shape of the cloud-droplet distribution. Collisional breakup of raindrops, which includes rebound effects, *i.e.,* all effects of coalescence efficiencies less than unity, is represented by a linear decrease of the self-collection rate, so that

$$\beta(D_m) = \begin{cases} 1 & D_m \leq 0.3 \times 10^{-3} \\ 1000 D_m - 1.1 & D_m > 0.3 \times 10^{-3} \end{cases}. \tag{23}$$

Non-equilibrium effects in auto-conversion and accretion are respectively modeled by the terms

$$\phi_{cc}(\varepsilon) = 1 + 600\frac{\varepsilon^{0.68}(1 - \varepsilon^{0.68})^3}{1 - \varepsilon} \quad \text{and} \quad \phi_{cr}(\varepsilon) = \left(\frac{\varepsilon}{\varepsilon + 5 \times 10^{-4}}\right)^4 \tag{24}$$

with

$$\varepsilon = r_r/(r_c + r_r). \tag{25}$$

Here ε is to be thought of as a non-dimensional time that measures the progression of the cloud water into rain water. The decomposition of the kinetic term into two additive terms is typical for bulk models, whereby the first term is identified with a process called auto-conversion, and the second represents accretion. Auto-conversion in most models does not depend on r_r. The r_r dependency of the auto-conversion term of $\mathcal{K}^{(sb)}$, through the ϕ_{cc} term, attempts to represent the effects of droplet spectral ripening (Cotton 1972; Lüpkes et al. 1989).

Sedimentation in SB is determined through a specification of the sedimentation velocities, which we write as

$$w_{n_r} = \frac{\int_{D_*}^{\infty} W_T(D)f(D)\,\mathrm{d}D}{\int_{D_*}^{\infty} f(D)\,\mathrm{d}D} = 9.65[1 - c_{sb}(1 + 600D_p)^{-(\mu+1)}] \tag{26}$$

$$w_{r_r} = \frac{\int_{D_*}^{\infty} W_T(D)D^3 f(D)\,\mathrm{d}D}{\int_{D_*}^{\infty} D^3 f(D)\,\mathrm{d}D} = 9.65[1 - c_{sb}(1 + 600D_p)^{-(\mu+4)}], \tag{27}$$

where W_T is the terminal velocity which depends only on the size of the drop, and c_{sb} is a constant, whose value along with other constants used by the scheme are given in Table 2. This formulation differs from the original proposal of SB.

Table 2: Constants for Microphysical Model.

Constant	Values
a_{sb}	1.408×10^{19}
b_{sb}	5.78
c_{sb}	1.015113

Table 3: Similarity constants for surface layer.

Constant	Value
Pr	0.74
κ	0.35
a_h	7.8
a_m	4.8
b_h	12.0
b_m	19.3

iii. Surface Fluxes To enforce the boundary conditions the model can either implement free slip or no-slip boundary conditions on the grid-scale tangential velocities, with free-slip being the default. These grid-scale quantities do however feel accelerations, or tendencies as a result of sub-grid scale fluxes which are parameterized. The model supports different methodologies for specifying the sub-grid fluxes at the lower boundary. They can be prescribed, calculated based on prescribed gradients, or prescribed surface properties. For the latter two similarity functions are chosen to relate the fluxes at the surface to the grid-scale gradients there. The similarity functions used by the model are as follows:

$$\Phi_h \equiv \frac{\kappa z}{\theta_*} \left(\frac{\partial \bar{\theta}}{\partial z} \right) = \begin{cases} Pr(1 + a_h\zeta) & \zeta > 0 \\ Pr(1 - b_h\zeta)^{-1/2} & \zeta \leq 0 \end{cases}$$

$$\Phi_m \equiv \frac{\kappa z}{u_*} \left(\frac{\partial \bar{u}}{\partial z} \right) = \begin{cases} (1 + a_m\zeta) & \zeta > 0 \\ (1 - b_m\zeta)^{-1/2} & \zeta \leq 0 \end{cases}$$

where

$$\zeta = z/\lambda \quad \text{and} \quad \lambda = \frac{\Theta_0}{g\kappa} \left(\frac{u_*^2}{\theta_*} \right)$$

is the Monin-Obukov length scale. The similarity constants in this formulation are listed in Table 3.

iv. Radiation The model allows for a range of different radiation types. As a default, calculations are done without radiation (iradtyp=0). For more explicit radiation treatment one can either use the simple radiation (iradtyp=2) following the gcss intercomparison or the full radiation (iradtyp=4) from Pincus and Stevens (2009). For simple radiation treatment, short- and longwave radiation will be computed as described in *src/rad_gcss.f90*. The full radiation package solves the radiative transfer with a delta-4 stream method. A particular treatment of radiation is available for the smoke cloud and the bellon case. The radiation treatment for the smoke cloud case can be used by setting iradtyp=2 and level=1. The bellon case has a specific radiation code as shown in the bellon_rad routine and can be used by setting iradtyp=3.

v. Land Surface Model The model can be used with an interactive land-surface scheme to calculate the fluxes between the land and atmosphere system. The scheme contains a surface layer and soil model following the approach used in the Dutch Atmospheric Large-Eddy Sumulation code (Heus (2010)). Fluxes are calculated interactively solving the energy budget at the surface for each grid cell. A four layer diffusive soil scheme is used to calculate temperature and soil moisture in every grid cell. We prescribe a mean deep soil temperature as a lower boundary of the model whereas soil and surface temperature and moisture are evolving in time. The land surface scheme can used in combination with the full radiation following Pincus and Stevens (2009). To assure a stable surface temperature the incoming long and shortwave radiation is averaged over a number of time steps (nradtime). The interactive calculation

of latent and sensible heat fluxes allows for multiple feedbacks in the coupled land-atmosphere system. This land surface setup has been tested against the Dutch Atmospheric LES (DALES) in a dry convective environment.

3. Numerics

a. *Time-stepping*

Time stepping is based on a Runge-Kutta third order method. An iterative method for the approximation of differential equations. A new timestep is computed using weighted supporting points (tendencies) for the calculation. The substeps done to determine any variable (ϕ) at the next timestep (ϕ^{n+1}) are calculated according to equations (28)-(30). The weighting factors are set to be $\alpha_i = \left(\frac{8}{15}, -\frac{17}{60}, \frac{3}{4}\right)$ and $\beta_i = \left(0, -\frac{15}{12}, -\frac{15}{12}\right)$.

$$\phi_*^n = \phi^n + \alpha_1 \frac{\partial \phi^n}{\partial t} \Delta t \tag{28}$$

$$\phi_{**}^n = \phi_*^n + \alpha_2 \frac{\partial \phi^n}{\partial t} \Delta t + \beta_2 \frac{\partial \phi_*^n}{\partial t} \Delta t \tag{29}$$

$$\phi^{n+1} = \phi_{**}^n + \alpha_3 \frac{\partial \phi_{**}^n}{\partial t} \Delta t + \beta_3 \frac{\partial \phi_*^n}{\partial t} \Delta t \tag{30}$$

The model employs a variable timestep, which is set so as to maintain a constant CFL maximum value bounded above by the value of the maximum timestep (dtlong in the NAMELIST file). If dtlong exceeds the maximum CFL value the actual timestep is scaled so that CFL value according to the new timestep is always 0.5.

b. *Computational Grid*
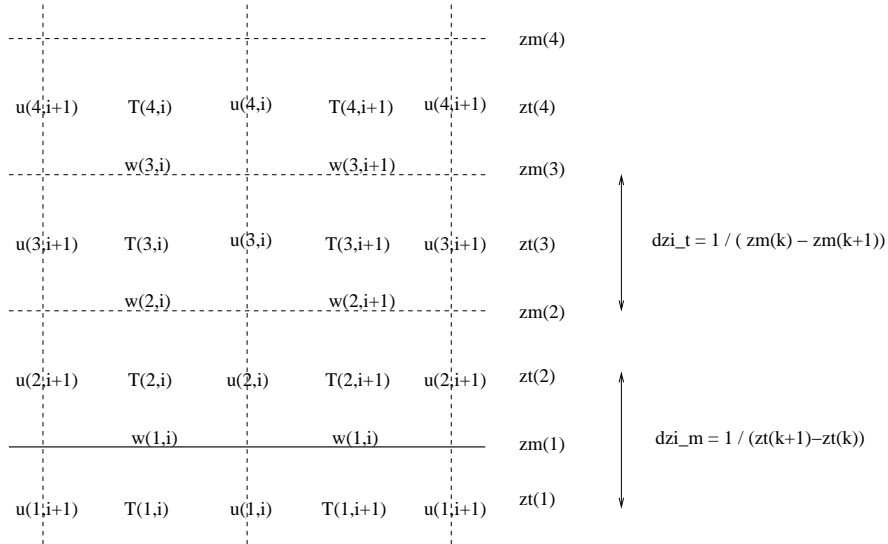

Figure 1: Schematic depiction of the model grid and where variables locate on it.

The grid is doubly periodic (in x-y) and bounded in the vertical, z. The vertical is spanned by a stretchable grid, the horizontal is tiled by uniform squares. Scalar advection is based on a directional-split monotone up winding method while momentum advection uses directionally-split fourth-order

centered differences. The model uses the Arakawa-C grid, which means that $u(k, i, j)$ lies $\frac{\Delta x}{2}$ meters to the right of $\theta_l(k, i, j)$. To state this more generally, velocities are staggered half a grid point up-grid (in the direction of the specific velocity component) of the thermodynamic and pressure points. Also note that the grid indexing has the z dimension first.[1] This k, i, j indexing is chosen in realization of the fact that many of the operations in the model are done column-wise. The grid configuration, and some height variables that are commonly used in the code (i.e., *zm, zt, dzm=dzi_m,* and *dzt=dzi_t*) are illustrated in a schematic drawing in Fig. 1.

c. *Pressure Solver*

Pressure is solved by a fractional step method so as to ensure that the velocities at the end of the timestep satisfy (3) to machine accuracy. The solver takes advantage of the periodicity in the horizontal to use 2-D FFTs to transform the Poisson-equation to a second order ODE in the vertical. Schematically

$$\frac{\partial^2 \pi}{\partial x_i^2} \longrightarrow (k^2 + l^2)\frac{d^2 \pi}{dz^2}, \tag{31}$$

where k and l denote the horizontal wave-numbers. The resultant ODE is then solved using a tri-diagonal solver.

d. *Parallelization Strategy*

Decomposition   The parallelization is performed by decomposing the domain into sub-domains consisting of columns in the x-y plane. This is a 2D decomposition in that the parallelization is along both the x and y dimensions. What results is N_p x-y columns where the number of grid points is evenly divided over the processors. N_p denotes the number of processors (columns) and N_x and N_y are the total number of unique x- and y-points. The way the memory is organized this has almost no impact on the code but requires that the columns have at least two unique x and y points. It also allows us to use domain-independent indexing, so that $j \in \{1, \ldots, N_y/N_p + 4\}$ where j is the $y-$index. The addend of four represents the contribution from the ghost points. The width of the ghost-points depends on the size of the largest stencil used for a differencing computation in the code. In our case the fourth order differences in the treatment of momentum fluxes. The effect of the ghost-strips is to increase the number of grid-points at the boundaries of the domain. This is required to calculate derivatives with the fourth order differences method as an example. The total number of grid-points, N_t is thus processor dependent.

2D parallelization allows us in principle to use $N_x N_y/4$ processors, i.e., more than 4 million with $N_x = N_y = 4096$. The normalized computational overhead associated with the ghost points can be measured by forming the ratio $R(N_p) = N_t(N_p)/N_t(1)$. For 2D decomposition with 2 ghost points deep:

$$R(N_p) = 1 + \frac{16(N_p - 1) + 4(N_x + N_y)\sqrt{N_p}}{N_x N_y + 16}$$

For $N_x = N_y = 2\sqrt{N_p} \gg 1$ this ratio approaches 7, although the communication overhead of such a large computation is more likely to be the bottleneck. I/O is currently handled by each processor.

Communication   With the current 2-D parallelization strategy global communications are needed to implement boundary conditions, compute domain integrals (such as means and co-variances), and calculate the FFTs. The latter is the most significant issue. The domain is first redistributed into strips (x-z

---

[1] Although given the way the model is written, this is merely a social contract among the various subroutines and thus could be changed.

plane).FFTs are computed in the $x-$direction (along a strip), then the domain is transposed into strips in the $y-$direction. After the transpose the FFTs are computed in the y-direction and then the vertical solver (tri-diagonal) solves the ODE (over z) in the transpose space. The inverse FFTs are then done in this transpose space, then the inverse transpose is performed before computing the inverse FFT along the strips in the x-direction. This strategy only requires four global communications per solve.

4. The Code

a. *Getting the Code*

The UCLA-LES Code is free for all to use, distribute, and call their own, following the guidelines of the gnu public license (http://www.gnu.org/licenses/). It is distributed through git, a free software source code management project. Subsequent developments of the code are available to its community here as well. The newest version of UCLA-LES will always be available at **http://git.gitorious.org/uclales**. To Download the newest UCLA-LES version make sure you have git installed on your system. Typing "git clone git@gitorious.org:uclales/uclales.git" in the command line will download the sources. You may want to check for updates by typing "git pull " in the command line. To check what has been changed since the last commit use "git status" and "git diff". You can also insert your private UCLA-LES version into git. For further information visit http://git.gitorious.org/uclales and see the git_uclales document in *doc* directory. Users of the code assume full responsibility for the results they produce. In addition users of the code are asked to share the burden of it's support.

b. *Organization*

The basic model is configured to solve an anelastic system of equations on the f-plane. It is written in F90/95, and is parallelized using a two-dimensional decomposition and MPI. Its primary form of output is NetCDF files, with FORTRAN binary output of history and restart files. The distribution is spread among four directories: *bin*, *doc*, *misc* and *src*. The code itself resides in *src* and is organized in F90 modules. These are described in Table 4. This directory also contains two subdirectories *seq* and *mpi* where the sequential or MPI modules are stored upon compilation. In addition rfft.F contains the Swartztrauber FFT routines which are called from the util module. Lastly a Makefile here formed by the master Makefile in *bin* defines the specific compilation/archive rules. To add new modules requires modification of this makefile.

The *bin* directory contains job control scripts and Makefiles which have to be adjusted to machine standards. The model is compiled from this directory (usually by typing make mpi or make seq respectively) and typically executed from here as well. The file NAMELIST defines any non-default input and is therefore the main control file.

The *doc* directory contains the latest version of this documentation. Also the gnu public license (also available at http://www.gnu.org/licenses/) which concerns the use of this UCLA-LES code can be found here. As described earlier the UCLA-LES is distributed through git. Here the git_uclales document gives an introduction how to use it in detail.

The *misc* directory is a catchall for other useful things, for instance *misc/initfiles* contains several NAMELIST files for idealized cases. Makefiles and jobscripts can be found in *misc/makefiles* and *misc/initfiles* respectively. *misc/synthesis* as well as *misc/scripts* contain other useful scripts. To start postprocessing *misc/analysis* suggests some simple NCL (the NCAR Command Language) scripts for plotting. NCL is a powerful data analysis , visualization, file-handling scripting language that is free and distributed by NCAR (National Center Of Atmospheric Research).

Table 4: Module F90 Files in *src* directory

Module	Contains
LES	Main program which calls a timing routine and the driver, as well as the driver subroutine and the subroutine which defines and reads the model NAMELIST file.
advf	Calculates the tendencies associated with scalar advection.
advl	Calculates the tendencies associated with momentum advection.
defs	Defines physical constants.
forc	Case specific forcings (radiation, subsidence, *etc.*).
grid	Definition of grid, allocation of memory and I/O management
init	Routines for processing input (either from a file or the NAMELIST), definition of basic state, initialization of fields, and definition of initial random perturbations.
lsvar	computes sst, div and winds for astex case (only when lsvar=true in NAMELIST)
ncio	Defines structure of ncdf output files.
mcrp	Bulk microphysical routines.
mpi_interface	Definition of MPI parameters and MPI routines for the domain decomposition (only when using MPI mode else seq_interface).
prss	Poisson solver, calculates the velocity tendencies associated with pressure gradients, also implements time-filter for leapfrog scheme and updates velocity.
rad_cldwtr	Calculates radiation properties from cloud water and effective radius.
rad_corkds	Reads gas concentrations and calculates radiative properties such as optical depth and absorption coefficients.
rad_d4strm	Computes radiative fluxes and optical properties for Rayleigh scattering.
rad_driver	Includes background soundings for atmospheric gases.
rad_gcss	Simple radiative parametrization for SW and LW fluxes (Delta-Eddigton approximation).
rad_rndnmb	Contains a random number generator.
rad_solver	Radiation solver.
sgsm	Subgrid scale solver.
srfc	Surface boundary condition routines.
stat	Routines for calculating, accumulating and outputting model statistics. Statistical output is provided through the course of a simulation and tends to be problem specific.
step	Time stepper. Also includes several routines for computing tendencies due to physical processes (Coriolis force, buoyancy) or boundary conditions (Rayleigh friction for sponge layer near lid). Updating of scalars is done here. CFL computations and timestep-regridding are also here.
thrm	Thermodynamic routines for calculating quantities like temperature, and cloud water, given the thermodynamic state of the model, i.e., $\theta_l, q_t, \rho_0, \pi_0, \Theta_0$.
util	A collection of basic utilities including boundary conditions, FFT calls, explicit array operations such as domain or slab averaging or covariances, the tri-diagonal solver, and some NetCDF utilities. Many of the routines in this module make active MPI calls.

c. *Compilation*

There are two ways of compiling the code: The preferred way uses CMake. CMake aims to resolve dependencies and compilation sequence automatically, allows for parallel compilation, and for quick switching between compilers or between debug and release mode. If CMake is not available on the system, some older example Makefiles are also provided.

i. CMake The first thing to setup is a config file with the paths to the various libraries. CMake will try to find the libraries on its own, but on many clusters the paths are non-standard, so we need to provide some pointers. Example files are available in the *config* directory. If any of these **.cmake* files matches your system, copy it to *default.cmake* (still in the *config* dir). If not, modify any of the files to create your own *default.cmake*.

Next thing is to create a build directory from where we will compile the code: *mkdir build && cd build* from the root dir of the code. To configure the code call cmake: *cmake ..* where ".." is the path back to the root directory of the code. After this, the code can be build with *make -j 4*, to use 4 processors while building the code. The resulting *uclales* binary can then be found in the *build* directory.

Changing from release mode (the default) to debug mode (with debug info, more restrictive checks, and less optimization) can be done with a cmake command line option: *cmake -D CMAKE_BUILD_TYPE=DEBUG ..* and *cmake -D CMAKE_BUILD_TYPE=RELEASE ..* respectively. Note that these options are persistent in that they will stay put for all compiling rounds, until being changed again by a cmake command.

ii. Make To compile the model type "make" in the the *bin* directory. This will build the default version of the model using the default architecture. To compile the code on different machines *bin/Makefile* must be adjusted. Examples of Makefiles are stored in *misc/makefiles*. Currently there are settings to compile on IBM, Macs with IBM/Motorola processors and the XLF compiler, and Linux. The code compiles and runs with G95 but our experiences to date with this compiler suggest that it produces executable which is a factor of two or more slower than commodity compilers.

The model requires the NetCDF libraries to build, and where they locate needs to be specified in *bin*. Our experiences with the most aggressive optimization has been generally positive on the IBMs, less so on the Mac. Fine tuning the optimization can lead to performance gains of 50% or more, but aggressive optimisation (O3 or greater on XLF compilers) should be checked. For computations with more than 128 points in a horizontal direction the code should be promoted to double precision, if only to yield better defined global integrals. One such integral that ends up being important is the mean buoyancy which must be subtracted from the local buoyancy so as to not cause any mean accelerations.

d. *Specialized model configurations*

Perhaps the best way to learn how to configure the model for different problems is to look at the configuration templates in the *misc* directories. Here sub-directories (*e.g.,* cumulus, gcss_dycoms, etc.,) contain substitute forcing, statistical and other modules, as well as alternate NAMELIST files. These are designed to run specific past cases and produce output required by them. Looking over how this is done in the code could provide an example of how to set up your own case, and statistical output. Starting from a case that is close to your desired objectives would naturally be the most straightforward way to proceed.

5. Running the Model

To run the model simply type the name of the executable (usually les.seq for sequential or les.mpi for parallel execution), otherwise one can submit it using a batch scheduler. The latter is almost always

necessary in parallel programming environments. Runscripts to schedule the job using IBM Loadleveler or IBM Load Sharing protocols are provided in the *misc/jobscripts* directory.

a. *The NAMELIST*

Model execution can be controlled by NAMELIST parameters. If a NAMELIST parameter does not appear in the NAMELIST file for a particular instance of the model execution, then the default value for that variable is assumed. In Table 5 we list the NAMELIST variables, their default values, the module in which they locate, and specialized behavior which can be obtained by specifying non-standard NAMELIST values.

The execution is controlled by a number of model parameters which are given default specifications in the code. These specifications can be modified in the NAMELIST file so as to allow multiple execution without recompilation. The full NAMELIST is defined in the LES.F90 subroutine and is described, along with default parameter values, in Table 5.

Table 5: NAMELIST variables and default values

Variable	Module	Default Value	Comments
nxp	grid	132	total number of x points ($N_y + 4$)
nyp	”	132	total number of y points ($N_y + 4$)
nzp	”	105	total number of z points
nxpart	”	true	2D domain decomposition
deltax	”	35.0 m	grid spacing in x-direction
deltay	”	35.0 m	grid spacing in y-direction
deltaz	”	17.5 m	grid spacing in z-direction
dzrat	”	1.0	grid stretching ration
dzmax	”	1200 m	height at which grid-stretching begins
dtlong	”	10 s	maximum timestep
nfpt	”	10	number of levels in upper sponge layer
distim	”	300 s	minimum relaxation time in sponge layer
th00	”	288	basic state potential temperature
igrdtyp	”	1	control parameter for selecting vertical grid
			1 = using nzp, deltaz, dzrat, dzmax
			2 = Tschebyschev grid
			3 = grid supplied via zm_grid_in
iradtyp	”	0	control parameter for selecting radiation model
			1,2,3 = case specific (see forc.f90)
			4 = delta-4 stream radiative transfer
			5 = surface radiation
lrad_ca	”	false	Perform clear air radiation calculations
isfctyp	”	0	control parameter for surface type
			0 = prescribed fluxes in dthcon, drtcon
			1 = prescribed gradient in dthcon, drtcon
			2 = sea surface ($q_{surf} = q_{sat}(SST)$)
			3 = sea surface ?
			4 = Variable $T_{surface}$ for constant buoyancy flux
			5 = Interactive land surface scheme
sfc_albedo	”	0.05	Surface albedo
naddsc	”	0	number of additional scalars
CCN	”	150×10^6	cloud droplet mixing ratio
expnme	”	Default	experiment name
filprf	”	x	file prefix for use in constructing output files
runtype	”	INITIAL	type of run ('INITIAL' or 'HISTORY')
level	”	0	0 = heat (θ) only
			1 = + water vapor (q_v)
			2 = + liquid water (q_l)
			3 = + rain (q_r)
			4 = + ice, snow, graupel (q_i, q_s, q_g)
			5 = + two-moment scheme
umean	”	0 m/s	Galilean transformation
vmean	”	0 m/s	Galilean transformation
lcouvreux	”	false	Couvreux decaying scalar
lwaterbudget	”	false	Liquid water budget diagnostics (level=3)
ipsflg	init	1	control parameter for input sounding ps

Table 5: NAMELIST variables and default values

Variable	Module	Default Value	Comments
			0 = pressure in hPa
			1 = meters, with ps(1) = p_{sfc}
itsflg	”	1	control parameter for input sounding *ts*
			0 = θ, 1 = θ_l
irsflg	”	1	control parameter for input sounding *rts*
			0 = q_t calculated from RH provided in *rts*
			1 = input *rts* in $g\ kg^{-1}$
us	”	n/a	input zonal wind sounding (max 500 points)
vs	”	n/a	input meridional wind sounding (max 500 points)
ts	”	n/a	input temperature sounding (max 500 points)
rts	”	n/a	input humidity sounding (max 500 points)
ps	”	n/a	input pressure sounding (max 500 points)
iseed	”	0	random seed
zrand	”	200 m	height below which random perturbations are added
mag_pert_t	”	0.2 K	magnitude of temperature pertubations
mag_pert_q	”	$5 \times 10^{-5} kg/kg^{-1}$	magnitude of moisture pertubations
hfilin	”	test.	name of input history file for HISTORY starts (xxx.)
lhomrestart	”	false	homogenize fields after restart
timmax	step	18000 s	final time of simulation
wctime	”	1e10 s	wall-clock limit
frqhis	”	9000 s	history write interval
frqanl	”	3600 s	analysis write interval
frqcross	”	3600 s	cross section write interval
istpfl	”	1	print interval for timestep info
corflg	”	false	coriolis acceleration
radfrq	”	0	radiation update interval
strtim	”	0	UTC of model time
cntlat	”	31.5° N	model central latitude
case_name	”	astex	specify case name (rico, astex, bomex, ..)
lsvarflg	”	false	reads large scale forcings from the file lscale_in
div	”	$0\ s^{-1}$	divergence
sst	”	292 K	(sea) surface temperature
lanom	”	false	...
tau	”	900 s	decay time scale Couvreux scalar
ltimedep	modtimedep	false	time dependant surface and large scale forcings
lstendflg	forc	false	large scale advective tendencies (file lstend_in)
lmtr	advf	3	limiter in flux-limited scalar advection
			0=no limiter, 1=minmod, 2=superbee
			3=mc, 4=van leer
advm	advl	4	momentum advection scheme
			2=2nd order centered
			4=2nd order centered
csx	sgsm	0.23	Smagorinsky Coefficient
prndtl	”	1/3	Prandtl Number (if less than zero no sgsm for scalars)
clouddiff	”	-1	Additional diffusion outside clouds

Table 5: NAMELIST variables and default values

Variable	Module	Default Value	Comments
ubmin	srfc	0.20	minimum u for u_* computation
zrough	”	0.01	momentum roughness height (if less than zero use Charnock relation)
dthcon	”	100 Wm^{-2}	itsflg=0: surface sensible heat flux
			itsflg=1: surface temperature gradient
drtcon	”	0 Wm^{-2}	itsflg=0: surface latent heat flux
			itsflg=1: surface mixing-ratio gradient
rh_srf	”	1.	surface relative humidity
drag	”	-1	optional prescribed drag coefficient
lhomflx	”	false	homogenize surface fluxes
fixed_sun	rad_driver	false	fix solar zenith angle
u0	”	n/a	cos(solar zenith angle) for fixed_sun=true
rad_eff_radius	”	1	fix for the cloud drop effective radius
cloud_type	mcrp	2403	Icemicro settings
lrandommicro	”	false	Do the microphysical terms in random order or not
microseq	”	{1,2,..,23}	Specify the order of the microphysical terms
timenuc	”	60	Ice nucleation time scale
nin_set	”	1700	Ice nuclei number
lpartdrop	”	false	...
SolarConstant	defs	1365 Wm^{-1}	Solar constant
ssam_intvl	stat	30 s	statistics sampling interval
savg_intvl	”	1800 s	statistics averaging interval
lcross	modcross	false	cross sections
dtcross	”	60 s	frequency cross sections
lxy	”	false	xy output
lxz	”	false	xz output
lyz	”	false	yz output
xcross	”	0 m	location of x slice
ycross	”	0 m	location of y slice
zcross	”	0 m	location of z slice (max 10 points, z>0), or:
			-1 = at height maximum buoyancy variance
			-2 = at cloud base
			-3 = at lifting condensation level
crossvars	”	see modcross.f90	list of output variables
prc_lev	”	-1	Output levels for the precip crosssections
lpartic	particles	false	Lagrangian particles
lpartsgs	”	false	sub-grid scheme particles
lrandsurf	”	false	randomize particles near surface
lpartstat	”	false	bin-average particle statistics
lpartdump	”	false	raw (netcdf) particle analysis files
frqpartdump	”	3600 s	frequency of writing analysis files
lpartdumpui	”	false	write velocities to analysis
lpartdumpth	”	false	write potential temperatures to analysis
lpartdumpmr	”	false	write mixing ratios to analysis
ldropstart	”	0 s	...

Table 5: NAMELIST variables and default values

Variable	Module	Default Value	Comments
lsync	modnetcdf	false	switch for buffering or immediate (much slower) IO in the netcdf files
deflate_level	"	0	NetCDF compression factor
lnudge	modnudge	false	nudging of wind and scalars to predefined profiles
tnudgefac	"	1	nudging time scale
qfloor	"	-1	(CGILS parameter) below zfloor, qt will be kept above this value
zfloor	"	1200 m	(CGILS parameter) below this value, qt will be kept above qfloor
znudgemin	"	-1	lower bound of the transition layer between free development and nudged atmoshpere
znudgeplus	"	-1	upper bound of the transition layer between free development and nudged atmoshpere
lnudgebound	"	false	...

To run a specific case one can copy the appropriate NAMELIST from *misc/initfiles* (see list of available NAMELIST files below). One may want to adjust parameters such as e.g. filprf, dtime, timmax, iradtyp,level and others before running the model. Here the use of the NAMELIST allows to change properties without recompiling the model. As an example, the parameter case_name in the NAMELIST file can be used to set large scale forcings for a specific case. Currently available case_names are: rico, bomex and atex.

- **namelist_astex**: The Astex case.

- **namelist_cumulus**: Namelist to reproduce the idealized cumulus cases reported in Stevens, JAS (2007). Requires the generation of a sound_in file with bstate.f95.

- **namelist_drycbl**: Idealized dry CBL consisting of a layer with initially uniform stratification and constant forcing.

- **namelist_dycm01**: The DYCOMS GCSS RF01 case, requires the generation of a sound_in file with bstate.f95.

- **namelist_dycm02**: The DYCOMS GCSS RF02 case, requires the generation of a sound_in file with bstate.f95, as well as the generation of zm_grid_in and zt_grid_in files uzing zgrid.gcss9.f.

- **namelist_rico**: The RICO GCSS composite case.

- **namelist_smoke**: The RICO GCSS smoke case.

b. *Output*

In addition to standard output, the model writes four types of files, all of which are controlled by options in the NAMELIST file, and the nature of the statistical routines in module *stat*.

Standard output: A number of fields are written to standard output. These include information about how the model is configured and how long a timestep is taking. Users may want to look at standard error as well. These information can be found in the $(filprf).time.out and $(filprf).time.err file respectively.

Where "time" is the time in seconds of the simulation and $(filprf) is the string associated with *filprf* in the NAMELIST file.

Analysis file: This NetCDF file contains space-time volumes that are useful for doing data analysis on select three-dimensional fields and are output periodically. In sequential runs this is a single file with the name $(filprf).nc, in parallel runs this consists of N_p (number of processors) files, one for each sub-domain with the name $(filprf).########.nc where ######## denotes the sub-domain number. The first four digits of the sub-domain number describe the processor number in x-direction (counting up from 0000) and the last four digits describe the processor number in y direction (counting up from 0000). These data are redundant with the history files, but less dense and in NetCDF, which allows for more frequent, output.

Profile statistics: Profile statistics are output in a NetCDF file called $(filprf).ps.nc for sequential or N_p files, one for each sub-domain with the name $(filprf).ps.########.nc for parallel runs. In parallel runs N_p profiles statistic files can be reduced to one file valid for the whole domain by using the reduce.ncl script in *misc/synthesis*. This file than contains profile statistics averaged over the averaging interval, with the number of samples determined by savg_intvl/ssam_intvl (see Table 5). This file is often used to plot profile statistics.

The ability of the model to calculate statistics on the fly can lead to more economical output and more accurate statistics. Our primary motivation for doing this is,however, that in general it is very important to use the same algorithm to calculate statistics (say fluxes for instance) as is used by the model to timestep the field. Given that, one might as well do the averaging during the course of a run. This method of averaging also makes it easier to generate finer grained statistics.

Temporal Statistics: This is a netCDF file called $(filprf).ts.nc for a sequential run or N_p files, one for each sub-domain with the name $(filprf).ts.########.nc for parallel runs. To reduce the number of files for parallel runs the reduce.ncl script mentioned above can be used as well. This file than contains selected time-series statistics which can be useful for getting a fine-grained view of the evolution of a calculation. Note that the parallel statistics are often computed only over a sub-domain and deriving the appropriate domain averaged quantity can be difficult (i.e. conditional averages).

History files: Fortran binary files which are given the name ####_####.(filprf)h.time where "time" is the time in seconds of the history write. ####_#### denotes the sub-domain number as described for the Analysis file and $(filprf) is the string associated with *filprf* in the NAMELIST file (only in parallel runs). History files contain the necessary data to restart the model from a given time and integrate it forward. The history write interval can be specified in the NAMELIST file with the variable frqhis. If you run the model for two hours and write a history file every hour (frqhis=3600s), you should be able to generate the data of the second hour identically by restarting the model from the history file, $(filprf)h.3600s written at the end of the first hour and integrating forward for an hour. In addition other types of history files can be written. $(filprf).iflg is written if the model is stopped due to a CFL violation (timestep has to be shorter than advective timescale); $(filprf).R at the first timestep when executed with *runtype* set to HISTORY; $(filprf).rst is the history state at the point when statistical averages are output (i.e., every *savg_intvl* seconds this file is overwritten with the current state). Restarting from this file helps restart the model form the latest data.

c. *Post-processing:*

I perform almost all of my post-processing using NCL (the NCAR Command Language). This is a powerful data analysis, visualization, file-handling scripting language that is free and distributed by

NCAR and handles NetCDF data intuitively. In the *misc/analysis* directory are some NCL files I use to process data. Similarly in *misc/synthesis* one should find the script reduce.ncl, which is used to reduce statistical (########.ps.nc and ########.ts.nc) files written over many sub-domains to one file valid for the entire domain.

Other Useful Scripts: *misc/synthesis/rename.csh* is used to rename all the files produced by a run. *misc/synthesis/call_mss.csh* invokes *misc/scripts/mss.csh* to transfer files to the NCAR Mass storagefacility. *misc/scripts/resubmit.csh* resubmits jobs after successful termination by changing the NAMELIST and calling the job scheduler. It was designed for the IBM SP systems. In *misc/analysis* examples of plotting scripts are shown. Generic scripts to plot files using NCL with command line arguments, i.e., plotfld.ncl, or a csh script plotfld.csh which invokes it.

d. *Debugging:*

My preferred way to debug the model is to track the evolution of the model state using print statements. I usually insert these between subroutine calls to specific processes in the t_step routine in Module step so as to isolate problems. When debugging it is useful to have some idea of how physical variables relate to model variables, which is the purpose of Table 6.

Table 6: Model variables

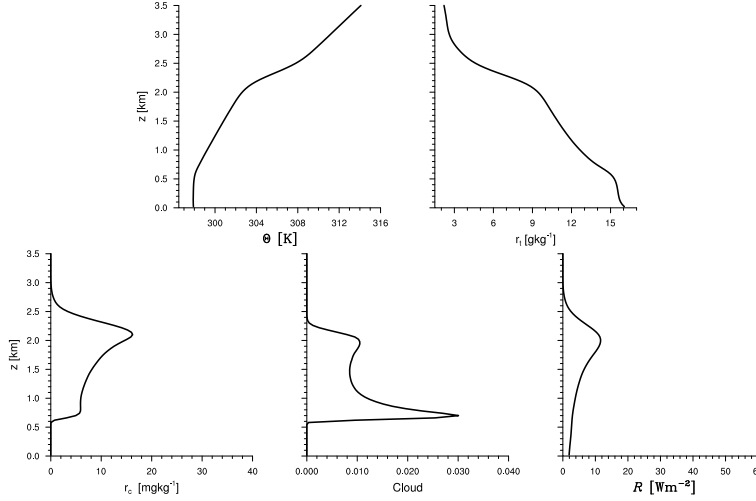| Array	Dimensionality	Field
a_xp,a_xt1,a_xt2	4D	Data arrays used to summarize variables
a_up,a_vp,a_wp	3D	u^n, v^n, w^n
a_ut,a_vt,a_wt	”	$\partial_t u$, $\partial_t v$, $\partial_t u$
a_tp,a_tt	”	Liquid water potential temperature, $\theta_l'^{\,n}$, $\partial_t \theta_l$
a_rp,a_rt	”	Total water mixing ratio r_t^n, $\partial_t r_t$
a_rpp,a_rpt	”	Rain mass mixing ratio r_r^n, $\partial_t r_r$ (for level 3)
a_npp,a_npt	”	Rain number mixing ratio, n_r^n, $\partial_t n_r$ (for level 3)
a_theta	”	Potential temperature, θ (diagnosed from model state)
rc,rv	”	Condensate and vapor mixing ratio r_c, r_v (note that r_c can be either the cloud or total condensate mixing ratio depending on when it is accessed)
press, a_pexnr	”	Pressure and Exner function (p, π respectively)
a_scr1, a_scr2	”	Three dimensional scratch arrays
a_ustar, a_tstar, a_rstar	2D	Surface scales, u_*, θ_*, r_* respectively
uw_sfc, vw_sfc, ww_sfc	”	Surface momentum fluxes, $\overline{u'w'}$, $\overline{v'w'}$, $\overline{w'w'}$ respectively.
wt_sfc, wq_sfc	”	Surface thermodynamic fluxes, $\overline{w'\theta'}$, $\overline{w'r'}$ respectively.
precip	”	Precipitation flux
dn0	1D	Basic state density, $\rho_0(z)$.
xt, yt, zt	”	Position of thermodynamic points
xm, ym, zm	”	position of momentum points
dzi_t	”	$1/(z_m(k) - z_m(k-1))$
dzi_m	”	$1/(z_t(k+1) - z_t(k))$

Figure 2: Thermodynamic profiles showing θ_l, r_t, r_c, core cloud fraction and rain rate (in energetic units) averaged over the last four hours of a 24 hour simulation.

6. Examples

In this section we show some basic profiles for some of the basic cases. By comparing your simulations with these you can get an idea if the model is behaving as it should. To help in these comparisons, sample ps and ts files are provided for the smoke, rico and dry CBL (dcbl) cases in the sub-directory *doc/sample_output*.

a. *RICO*

The run was performed in two stages on 64 processors (two virtual processors per real processor) on the IBM power5 BlueVista Machine. It took about 4.5 hours of real time to compute 24 hours of simulated time. The output was processed by first reducing the ts and ps files, then plotting. An example of the thermodynamic state averaged over the last four hours of the simulation is shown in Fig. 2. These results will differ slightly from those submitted as part of the GCSS RICO intercomparison because of slight changes used in the microphysics in the present case, namely drop breakup and ventilation effects were included.

b. *Dry CBL*

To run this case we used the NAMELIST file from the *misc/original* directory. The run was performed on the IBM power5 BlueVista Machine. It took less than an hour to finish four hours of simulated time. The evolution of this run is shown in Figure 3 by the profiles of θ at half hour intervals, where each profile is a 15 minute average.

c. *Smoke*

Finally in Figure 4 we show the evolution of the smoke cloud case. For this plot we show the half hour averaged profiles for the periods ending at 2 and 4 hrs. The initial state is also shown by the solid line. What we see in the mean profiles is the expected propagation of the smoke layer into the overlying fluid, accompanied by the dilution of the smoke layer. The slight instability at the top of the smoke layer (θ decreasing with height) is the signature of the radiative cooling active in this case.
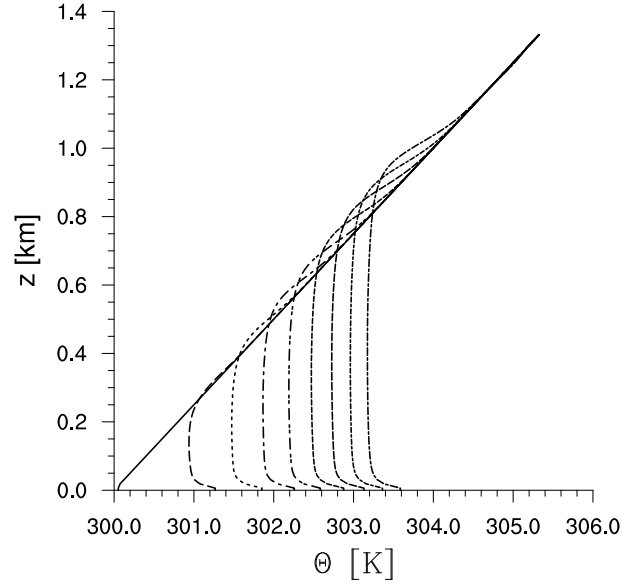
Figure 3: Mean potential temperature profile for sample (default) dry convective boundary layer simulation. Profiles show averages over 15 minutes plotted at 30 min intervals, with initial state (actually state at the end of the first timestep) shown by solid line.
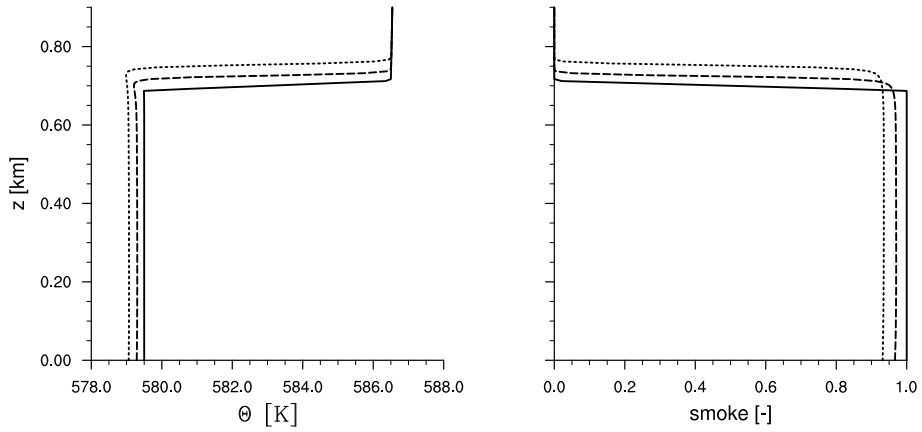

Figure 4: Mean potential temperature profile for smoke cloud simulation. Shown are profiles of θ and smoke concentration averaged over 30 minutes plotted at 2 hr intervals, with initial state (actually state at the end of the first timestep) shown by solid line.

References

Cotton, W. R., 1972: Numerical simulation of precipitation development in supercooled cumuli-part I. *Mon. Wea. Rev.*, **100**, 757–763.

Long, A. B., 1974: Solutions to the droplet coalescence equation for polynomial kernels. *J. Atmos. Sci.*, **31**, 1040.

Heus, T. and van Heerwaarden, C. C. and Jonker, H. J. J. and Pier Siebesma, a. and Axelsen, S. and van den Dries, K. and Geoffroy, O. and Moene, a. F. and Pino, D. and de Roode, S. R. and Vilà-Guerau de Arellano, J., 2010: Formulation of the Dutch Atmospheric Large-Eddy Simulation (DALES) and overview of its applications. *Geoscientific Model Development*, **3**, 415-444.

Lüpkes, C., K. D. Beheng, and G. Doms, 1989: A parameterization scheme simulating warm rain formation due to collision/coalescence of water drops. *Contributions to Atmospheric Physics*, **62**, 289–306.

Milbrandt, J. A. and M. Yau, 2005: A multimoment bulk microphysics parameterization. part I: analysis of the role of the spectral shape parameter. *J. Atmos. Sci.*, **62**, 3051–3064.

Ogura, Y. and N. A. Phillips, 1962: Scale Analysis of Deep and Shallow Convection in the Atmosphere. *J. Atmos. Sci.*, **19**, 173–179.

Pincus, R. and B. Stevens, 2009: Monte Carlo Spectral Integration: a Consistent Approximation for Radiative Transfer in Large Eddy Simulations. *Journal of Advances in Modeling Earth Systems*, **1**.

Seifert, A. and K. D. Beheng, 2001: A double-moment parameterization for simulating autoconversion, accretion and self collection. *Atmos Res*, **59-60**, 265–281.

Seifert, A., 2008: On the Parameterization of Evaporation of Raindrops as Simulated by a One-Dimensional Rainshaft Model. *J. Atmos. Sci.*, **65**, 3608–3619.

Stevens, B., C.-H. Moeng, A. S. Ackerman, C. S. Bretherton, A. Chlond, S. de Roode, J. Edwards, J.-C. Golaz, H. Jiang, M. Khairoutdinov, M. P. Kirkpatrick, D. C. Lewellen, A. Lock, F. Müller, D. E. Stevens, E. Whelan, and P. Zhu, 2005: Evaluation of large-eddy simulations via observations of nocturnal marine stratocumulus. *Mon. Wea. Rev.*, **133**, 1443–1462.

Stevens, B., C.-H. Moeng, and P. P. Sullivan, 1999: Large-eddy simulations of radiatively driven convection: sensitivities to the representation of small scales. *J. Atmos. Sci.*, **56**, 3963–3984.

Stevens, B. and A. Seifert, 2008: On the sensitivity of simulations of shallow cumulus convection to their microphysical representation. *J. Meteorol. Soc. Japan*.